

Intrinsic Differences in the Response of the Human Lutropin Receptor *Versus* the Human Follitropin Receptor to Activating Mutations*

Received for publication, April 26, 2007, and in revised form, June 21, 2007. Published, JBC Papers in Press, July 2, 2007, DOI 10.1074/jbc.M703500200

Meilin Zhang[‡], Ya-Xiong Tao^{‡1}, Ginny L. Ryan^{‡2}, Xiuyan Feng[‡], Francesca Fanelli[§], and Deborah L. Segaloff^{‡3}

From the [‡]Department of Molecular Physiology and Biophysics, the University of Iowa Carver College of Medicine, University of Iowa, Iowa City, Iowa 52242 and the [§]Dulbecco Telethon Institute and Department of Chemistry, University of Modena e Reggio Emilia, Via Campi 183, 41100 Modena, Italy

In contrast to the human lutropin receptor (hLHR), very few naturally occurring activating mutations of the structurally related human follitropin receptor (hFSHR) have been identified. The present study was undertaken to determine if one aspect underlying this discrepancy might be a general resistance of the hFSHR to mutation-induced constitutive activity. Five different mutations were introduced into both the hLHR and hFSHR (four based on activating mutations of the hLHR gene, one based on an activating mutation of the hFSHR gene). Our results demonstrate that hFSHR constitutively activating mutants (CAMs) were not as active as hLHR CAMs containing the comparable mutation. Furthermore, although all hFSHR CAMs exhibited strong promiscuous activation by high concentrations of the other glycoprotein hormone receptors, hLHR CAMs showed little or no promiscuous activation. Our *in vitro* findings are consistent with *in vivo* observations of known pathophysiological conditions associated with hLHR CAMs, but not hFSHR CAMs, and with promiscuous activation of hFSHR CAMs, but not hLHR CAMs. Computational experiments suggest that the mechanisms through which homologous mutations increase the basal activity of the hLHR and the hFSHR are similar. This is particularly true for the strongest CAMs like L460^(3,43)R. Disparate properties of the hLHR *versus* hFSHR CAMs may, therefore, be due to differences in shape and electrostatics features of the solvent-exposed cytosolic receptor domains involved in the receptor-G protein interface rather than to differences in the nature of local perturbation at the mutation site or in the way local perturbation is transferred to the putative G protein binding domains.

The LH receptor (LHR)⁴ and FSH receptor (FSHR), collectively termed the gonadotropin receptors, are G protein-coupled receptors whose primary role is mediation of the signal transduction by pituitary LH or placental hCG (LHR) or pituitary FSH (FSHR) in the gonads. The LHR and FSHR are each composed of a serpentine region containing the seven transmembrane helices typical of G protein-coupled receptors as well as a large extracellular domain that confers the high affinity binding of hormone (1, 2). The gonadotropin receptors are members of the leucine-rich glycoprotein receptor subfamily of rhodopsin-like G protein-coupled receptors (3). The gonadotropin receptors of human origin are highly homologous, with the greatest degree of amino acid conservation within the transmembrane helices. Recent crystallographic studies on human FSH (hFSH) bound to the extracellular domain of the hFSHR have tremendously advanced our understanding of the mechanism of hormone binding to the gonadotropin receptors (4). The entire receptor complexed with ligand has yet to be crystallized, however, and it is still unclear how the binding of hormone to the extracellular domain of the gonadotropin receptor causes stabilization of the serpentine region in an active conformation that causes stimulation of G proteins, primarily G_s.

In the past several years, numerous mutations of the hLHR gene have been identified in young boys with gonadotropin-independent precocious puberty (see Refs. 5 and 6 for reviews). Consistent with the clinical phenotype, studies utilizing heterologous cells transfected with the mutant hLHRs confirm that the mutations cause the constitutive activation of G_s in the absence of bound hormone. Interestingly, of all the known hLHR constitutively activating mutants (CAMs), only D578^(6,44)H⁵ has been found to be associated with Leydig cell tumors (8, 9). Although it was originally hypothesized that the D578^(6,44)H mutant uniquely caused activation of the phospholipase C signaling pathway (8), more recent studies suggest that the G proteins and second messenger pathways activated by

* These studies were supported by National Institutes of Health Grant HD22196 (to D. L. S.) and Telethon Italy Grant S00068TELU (to F. F.). The costs of publication of this article were defrayed in part by the payment of page charges. This article must therefore be hereby marked "advertisement" in accordance with 18 U.S.C. Section 1734 solely to indicate this fact.

¹ Present address: Dept. of Anatomy, Physiology, and Pharmacology, College of Veterinary Medicine, Auburn University, Auburn, AL 36849.

² Present address: Dept. of Obstetrics and Gynecology, University of Iowa Carver College of Medicine, University of Iowa, Iowa City, IA 52242.

³ To whom correspondence should be addressed: Dept. of Molecular Physiology and Biophysics, 5-470 Bowen Science Bldg., University of Iowa, Iowa City, IA 52246. Tel.: 319-335-7850; Fax: 319-335-7330; E-mail: deborah-segaloff@uiowa.edu.

⁴ The abbreviations used are: LHR, LH receptor; FSHR, FSH receptor; hFSH and hFSHR, human FSH and FSHR, respectively; CAM, constitutively activating mutant; OHSS, ovarian hyperstimulation syndrome; WT, wild type; SAS, solvent-accessible surface area.

⁵ The amino acid numbering in superscript is that proposed by Ballesteros and Weinstein (7). In this nomenclature, the first number indicates the helix and the numbers thereafter indicate the position of the helical residue relative to the most highly conserved residue within that helix, which is denoted as 50.

Activating Mutations of the hFSHR

D578^(6.44)H are the same as those activated by other hLHR CAMs (10, 11). Computational modeling on the isolated wild type (WT) and constitutively active mutants of the hLHR suggests that ligand-independent activation of the hLHR involves changes in the interaction pattern of Arg-464^(3.50) of the highly conserved (E/D)R(Y/W) motif and the opening of a solvent-accessible crevice in the neighbors of this conserved arginine (12–15).

In contrast to the hLHR, very few naturally occurring activating mutations of the hFSHR have been described (16–20). Initially, one activating mutation of the hFSHR was identified in a hypophysectomized man exhibiting spermatogenesis (16). More recently, studies were undertaken to examine the hFSHR in women with a history of ovarian hyperstimulation syndrome (OHSS) during naturally conceived pregnancy. As was predicted, these women had mutations of the hFSHR gene that caused the receptor to inappropriately respond to the elevated concentrations of hCG that normally occur during pregnancy, resulting in excessive ovarian follicular growth (17–20). Interestingly, functional analyses of these hFSHR mutants expressed in heterologous cells revealed that they also exhibited elevated basal constitutive activities in the absence of any hormone. There did not appear to be any physiological abnormalities in these women outside of pregnancy; however, that could be associated with the constitutive activity of the hFSHR. Other studies specifically looking for activating mutations of the hFSHR gene did not uncover any. Thus, studies examining the hFSHR gene in granulosa cell tumors and in families with a history of nonidentical twins did not reveal any activating mutations of the hFSHR (21–23).

Interestingly, when the hFSHR was modified to contain a D^(6.44)G mutation, a substitution known to cause constitutive activation of the hLHR, it did not result in constitutive activation of the hFSHR (24, 25). These results suggest that the hFSHR may be more resistant to mutation-induced constitutive activity than the hLHR, thus potentially accounting for (at least in part) the relative paucity of naturally occurring mutations of the hFSHR that have been identified. However, in contrast to the D^(6.44)G mutation, introduction of the hLHR-activating mutation L^(3.43)R into the hFSHR was shown to cause significant hFSHR constitutive activation (26). A direct comparison, however, of the L^(3.43)R mutation in the hLHR *versus* the hFSHR was not performed. Therefore, it is not possible to conclude from these earlier, more limited studies whether or not the hFSHR is generally more refractory to mutation-induced constitutive activation than the hLHR. To examine this question in a more thorough and quantitative manner, the present studies were undertaken in which we have introduced several mutations known to cause activation of the hLHR into the hFSHR. The properties of the hFSHR mutants were determined and compared with the cognate mutants of the hLHR, and the structures of each of the mutants were predicted using computational molecular modeling.

MATERIALS AND METHODS

Plasmids and Reagents—The cDNAs for the WT hFSHR and hLHR and highly purified recombinant hFSH were generous

gifts from Ares Advanced Technology (Ares-Serono Group, Randolph, MA). Highly purified recombinant hTSH was purchased from Genzyme (Cambridge, MA). The specific activity for the hTSH was listed as 4–12 IU/mg. For the purposes of this study, a specific activity of 4 IU/mg was used for calculating the concentrations of hTSH. Pregnant mare serum gonadotropin (used to determine the nonspecific binding of ¹²⁵I-hFSH) and highly purified recombinant hCG were purchased from Dr. A. Parlow and the NIDDK, National Institutes of Health, National Hormone and Pituitary Program. Crude hCG (used to determine the nonspecific binding of ¹²⁵I-hCG) was purchased from Sigma.

The WT cDNAs for the hFSHR and hLHR were placed into pcDNA3.1(neo). The WT receptors, as well as all mutants thereof, were modified to contain a Myc epitope tag at the N terminus. Mutations were introduced using the PCR overlap method of site-directed mutagenesis (27, 28). The plasmids were prepared using the Qiagen Maxiprep kit (Qiagen, Valencia, CA), and the entire coding regions were sequenced by automated DNA sequencing (performed by the DNA Core Facility of the University of Iowa Carver College of Medicine).

Cells and Transfections—Human embryonic kidney (HEK) 293 cells were obtained from the American Type Tissue Collection (CRL 1573) and were maintained at 5% CO₂ in growth medium consisting of high glucose Dulbecco's modified Eagle's medium containing 50 μg/ml gentamicin, 10 mM HEPES, and 10% newborn calf serum. Cells for experiments were plated onto wells (24-well plates for experiments examining the potential promiscuous activation of hFSHR and hLHR CAMs, 6-well plates for all other experiments) that had been precoated for 45 min with 0.1% gelatin in calcium- and magnesium-free phosphate-buffered saline, pH 7.4. Cells were transiently transfected at 50–70% confluence following the protocol of Chen and Okayama (29), except that the overnight precipitation was performed in a 5% CO₂ atmosphere. Cells were then washed with Waymouth's MB752/1 medium modified to contain 50 μg/ml gentamicin and 1 mg/ml bovine serum albumin, after which fresh growth medium was added. The cells were used for experiments 24 h later. When transfecting cells with varying concentrations of plasmid containing receptor cDNA, the total amount of plasmid was kept constant with empty vector.

Hormone Binding Assays to Intact Cells—HEK293 cells were plated onto gelatin-coated wells and transiently transfected as described above. On the day of the experiment, cells were washed two times with warm Waymouth's MB752/1 containing 50 μg/ml gentamicin and 1 mg/ml bovine serum albumin. To determine the maximal binding capacity for hFSHR-expressing cells, the cells were then incubated for 1 h at room temperature in the same medium containing a saturating concentration of ¹²⁵I-hFSH (300 ng/ml final concentration) with or without an excess of unlabeled pregnant mare serum gonadotropin (220 IU/ml final concentration). For hLHR-expressing cells, ¹²⁵I-hCG (500 ng/ml final concentration) with or without crude hCG (50 IU/ml final concentration) was used. Two wells were used to determine total binding, and one well was used to determine nonspecific

		N-TER	
rhodopsin	M N G T E G P N F Y V P F S N K T G V V R S P F E A P Q Y Y L A E P		34
hFSHR	F D M T Y T E F D Y D L C N E V V D V T C S P K P D A F N P C E D I		359
		H1	
rhodopsin	W Q F S M L A A Y M F L L I M L G F P I N F L T L Y V T V Q		64
hFSHR	M G Y N I L R V L I W F I S I L A I T G N I I V L V I L T T		389
		IL1	
rhodopsin	H K K L R T		70
hFSHR	S Q Y K L T		395
		H2	
rhodopsin	P L N Y I L L N L A V A D L F M V F G G F T T T L Y T S L - -		99
hFSHR	V P R F L M C N L A F A D L C I G I Y L L L I A S V D I H T K		426
		EL1	
rhodopsin	- - Y F V F - -		105
hFSHR	S Q Y H N Y A I		434
		H3	
rhodopsin	- - - - T G C N L E G F F A T L G G E I A L W S L V V L A I E R Y V V V		139
hFSHR	D W Q T G A G C D A A G F F T V F A S E L S V Y T L T A I T L E R W V T I		471
		IL2	
rhodopsin	C K P M S - N F R F G E N		151
hFSHR	T H A M Q L D C K V Q L R		484
		H4	
rhodopsin	H A I M G V A F T W V M A L A C A A P P L V		173
hFSHR	H A A S V M V M G W I F A F A A A L F P I F		506
		EL2	
rhodopsin	G W S R Y I P E G M Q C S C G I D Y Y T P H E E T N N E		201
hFSHR	G I S S Y M K V - - - S I C L P M D I - - - D S P L S Q		528
		H5	
rhodopsin	S F V I Y M F V V H F I I P L I V I F F C Y G Q L V F		228
hFSHR	L Y V M S L L V L N - V L A F V V I C G C Y I H I Y L		554
		IL3	
rhodopsin	T V K E A A A - -		235
hFSHR	T V R N P N I V S		563
		H6	
rhodopsin	T Q K A E K E V T R M V I I M V I A F L I C W L P Y A G V A F Y I F T H		278
hFSHR	S S - S D T R I A K R M A M L I F T D F L C M A P I S F F A I S A S L K		598
		EL3	
rhodopsin	Q G S D F G P		285
hFSHR	V P L I T V S		605
		H7	
rhodopsin	I F M T I P A F F A K T S A V Y N P V I Y I M M N	H8	
hFSHR	K A K I L L V L F H P I N S C A N P F L Y A I F T	K Q F R N C M V T K N F R R D F F I	319 636

FIGURE 1. **Rhodopsin and hFSHR sequence alignment.** Shown is a sequence alignment between bovine rhodopsin (Protein Data Bank code 1U19 (31)) (*i.e.* template) and the hFSHR (target) that was employed for comparative modeling. The amino acid stretches 100–101, 106–107 and 236–242 have been deleted from the 1U19 template. The boxed sequences correspond to H8.

binding. The assay was terminated by washing the cells three times with cold Hanks' balanced salt solution modified to contain 50 $\mu\text{g}/\text{ml}$ gentamicin and 1 $\mu\text{g}/\text{ml}$ bovine serum albumin. The cells were then solubilized in 0.5 N NaOH, transferred to plastic test tubes with cotton swabs, and counted in a γ counter.

Determination of Intracellular cAMP Production—HEK293 cells were plated onto gelatin-coated wells and transiently transfected as described above. On the day of the experiment, cells were washed two times with warm Waymouth's MB752/1 containing 50 $\mu\text{g}/\text{ml}$ gentamicin and 1 mg/ml bovine serum albumin and placed into 1 ml of the same medium containing 0.5 mM isobutylmethylxanthine. After a 15-min preincubation at 37 °C, buffer alone (for basal cAMP levels) or hormone was added to give the final concentrations noted, and the cells were incubated for a further 60 min at 37 °C. The cells were then placed on ice, the medium was aspirated, and intracellular cAMP was extracted by the addition of 0.5 N perchloric acid containing 180 $\mu\text{g}/\text{ml}$ theophylline and measured by radioimmunoassay. All assays were performed with triplicate wells, and the cAMP in each well was determined in duplicate in the radioimmunoassay. Statistical analyses were performed with InStat (GraphPad Software, San Diego, CA). An unpaired *t* test was used to compare the hormone-stimulated cAMP concentrations with the basal concentration of cAMP in cells express-

ing a given receptor construct. A statistically significant difference was defined as $p < 0.05$.

Computational Modeling of the hFSHR—The initial hFSHR model was built by means of the comparative modeling software MODELER (30), using the latest rhodopsin structure as a template (*i.e.* Protein Data Bank code 1U19 (31)). The modeled sequence includes the transmembrane helices, the three intracellular loops (IL1, IL2, and IL3), the three extracellular loops (EL1, EL2, and EL3), and the 326–358 ectodomain sequence, which can be reasonably modeled based upon the N terminus of rhodopsin (Fig. 1). A modified rhodopsin template was employed in which the sequences 100–101 and 106–107 were deleted, which correspond to the H2/EL1 junction and the first two amino acids of H3, respectively. The sequence 236–242, corresponding to the C-terminal region of IL3, was deleted as well. During comparative modeling, α -helical restraints were imposed on the hFSHR sequences 420–427 and 434–441.

Using the sequence alignment shown in Fig. 1, 200 models were obtained by randomizing the Cartesian coordinates of the model through a random number uniformly distributed in an interval from -4 to 4 Å (30). Among the 200 models finally obtained, one model was selected that showed low restraint violations associated with high values of the 3D-Profile score, computed by means of the Protein Health module in the QUANTA 2000 package, and low numbers of main chains and side chains in nonallowed conformations and close contacts. This model was subjected to automatic and manual rotation of the side-chain torsion angles when in nonallowed conformations, leading to the input structure for energy minimization and molecular dynamics simulations. Energy minimization and molecular dynamics simulations were carried out by means of the CHARMM program (31, 32), using an implicit membrane-water model recently implemented (*i.e.* the GBSW module) (33). With respect to the physical parameters representing the membrane in the GB model, the surface tension coefficient (representing the nonpolar solvation energy) was set to 0.03 kcal/(mol \cdot Å 2). Furthermore, the membrane thickness centered at $Z = 0$ was set to 30.0 Å with a membrane smoothing length of 5.0 Å ($w_m = 2.5$ Å).

Minimizations were carried out using 1500 steps of steepest descent, followed by adopted basis Newton-Raphson minimization until the root mean square gradient was less than 0.001 kcal/mol Å. Two disulfide bridge patches were applied to Cys-

Activating Mutations of the hFSHR

TABLE 1

hFSHR constructs containing mutations corresponding to known hLHR activating mutations for constitutive activity

HEK293 cells were transiently transfected with one or more mutant hFSHRs and with varying concentrations of WT hFSHR (with total plasmid held constant with empty vector). Cell surface hFSHR and basal cAMP were measured within a given experiment. The cAMP levels of cells expressing a mutant hFSHR were compared with cells within that experiment that expressed similar levels of cell surface WT receptor as the mutant. In each experiment, the basal cAMP levels for a mutant were expressed relative to the expression-matched WT control. The data shown are the mean \pm S.E. of the normalized basal cAMP levels obtained in the indicated number of experiments. The hFSHR mutants shown in boldface type depict those whose basal levels of cAMP were >3 -fold higher than the expression-matched WT hFSHR cells.

hFSHR mutant	Corresponding hLHR CAM	hFSHR basal cAMP (mutant/WT)	<i>n</i>
A376 ^(1.46) V	A373 ^(1.46) V	1.84 \pm 0.33	7
M401^(2.43)T	M398^(2.43)T	3.60 \pm 0.53	9
V543 ^(5.41) L	V540 ^(5.41) L	1.47 \pm 0.20	11
I545^(5.46)L	I542^(5.46)L	4.53 \pm 1.45	6
A571 ^(6.34) V	A568 ^(6.34) V	1.98 \pm 0.34	5
M574 ^(6.37) I	M571 ^(6.37) I	2.19 \pm 0.46	5
A575 ^(6.36) V	A572 ^(6.36) V	2.95 \pm 0.64	5
I578 ^(6.41) L	I575 ^(6.41) L	2.49 \pm 0.85	4
T580^(6.43)I	T577^(6.43)I	5.41 \pm 0.76	6

338 and Cys-356 (in the ectodomain) and to Cys-442^(3.25) and Cys-517 (in EL2). Simulations without the disulfide bridge between Cys-338 and Cys-356 were carried out as well.

The all-atom parameter set was used. The lengths of the bonds involving the hydrogen atoms were restrained by the SHAKE algorithm, allowing an integration time step of 0.001 ps. The systems were heated to 300 K with 7.5-K rises every 2500 steps per 100,000 steps by randomly assigning velocities from the Gaussian distribution. After heating, the system was allowed to equilibrate for 100 ps. The secondary structure of the helix bundle was preserved by assigning distance restraints (*i.e.* minimum and maximum allowed distances of 2.7 and 3.0 Å, respectively) between the backbone oxygen atom of residue *i* and the backbone nitrogen atom of residue *i* + 4, except for prolines. The scaling factor of such restraints was 10, and the force constant at 300 K was 10 kcal/mol Å. The receptor amino acids, which were found in noncanonical α -helical conformations in the input structure, a condition inherited from the rhodopsin template, were not subjected to any intrabackbone distance restraints. The selected input structure was used to produce the hFSHR constitutively active mutants M401^(2.43)T, L460^(3.43)R, I545^(5.46)L, and T580^(6.43)I. WT and mutated structures were subjected to 1 ns molecular dynamics simulations, and the structures averaged over the 2000 structures constituting the entire 1 ns trajectories were considered for the analyses presented.

RESULTS

Screening of hFSHR Mutants for Constitutive Activity—Previous studies from our laboratory had shown that the hFSHR mutation hFSHR(L460^(3.43)R), corresponding to the activating L457^(3.43)R mutation of the hLHR, resulted in constitutive activation (26). In contrast, the hFSHR mutation hFSHR(D581^(6.44)G), corresponding to the activating D578^(6.44)G mutation of the hLHR, did not result in constitutive activation (24, 25). To more generally determine if the hFSHR is rendered constitutively active when known hLHR activating mutations are introduced, nine other naturally occurring activating mutations of the hLHR were introduced into the corresponding position of the hFSHR (Table 1). In

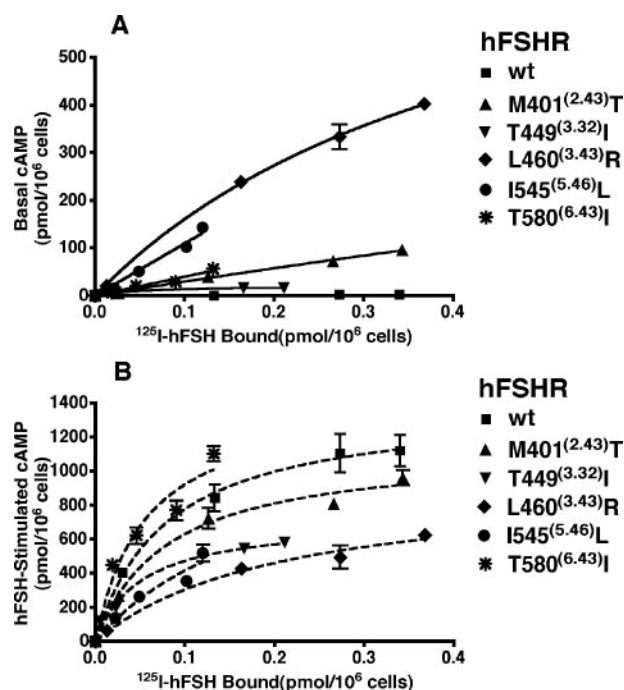


FIGURE 2. Basal and hFSH-stimulated cAMP in hFSHR constitutively active mutants. HEK293 cells were transiently transfected with increasing amounts of plasmids encoding the indicated WT or mutant hFSHRs. Plasmid concentrations were kept constant by the addition of empty vector pcDNA3.1(neo). In the same experiment, cell surface receptors, as measured by ¹²⁵I-hFSH binding assays to intact cells, and cAMP measurements were performed. cAMP levels were determined under basal conditions (A) or after stimulation with hFSH (300 ng/ml final concentration) (B). The data shown are from one representative experiment and depict the mean \pm S.E. of triplicate determinations within that experiment after subtracting the cAMP measured in cells expressing empty vector only. Similar results were obtained in three or more independent experiments.

these experiments, the basal cAMP levels in cells expressing the WT *versus* mutant hFSHR were analyzed in cells expressing similar levels of cell surface receptors. Most of these hFSHR mutants exhibited extremely low levels of constitutive activity. However, cells expressing the hFSHR mutants M401^(2.43)T, I545^(5.46)L, and T580^(6.43)I displayed basal cAMP levels that were more than 3 times greater than cells expressing the WT hFSHR. These three hFSHR mutants were chosen for further characterization and compared with the known hFSHR-activating mutant L460^(3.43)R (26) as well as to the naturally occurring activating hFSHR mutant T449^(3.32)I that had been identified in a woman with OHSS in a naturally conceived pregnancy (17).

Basal and hFSH-stimulated Activities of hFSHR CAMs—These five activating hFSHR mutants were compared with each other and with the WT hFSHR to measure their relative constitutive activities and hormone-stimulated activities. To obtain a more quantitative assessment of the activities of the different receptors and to mitigate differences in receptor expression, we analyzed cAMP production in cells expressing a wide range of cell surface receptor levels. Therefore, the data in Fig. 2 depict the activities of the different receptor constructs analyzed within the same experiment and as a function of different receptor densities. The fact that the curves for some mutants terminate sooner than others reflects the relatively low cell surface expression of those mutants (*i.e.* T449^(3.32)I

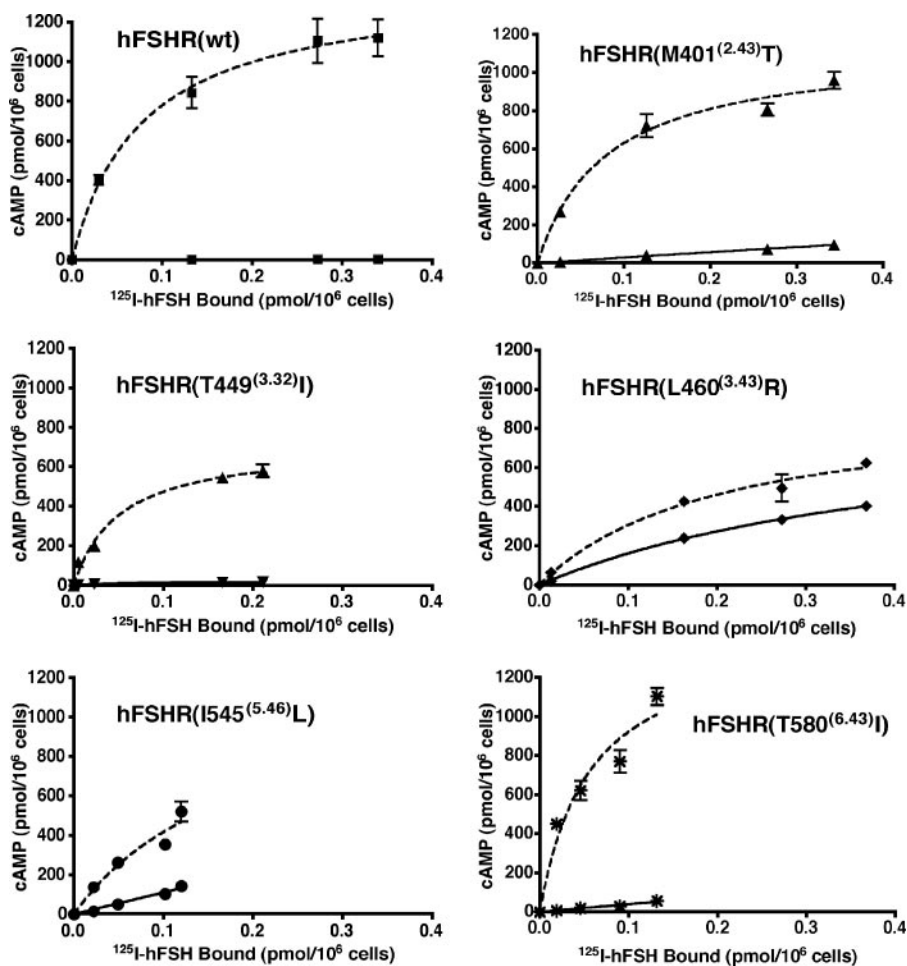


FIGURE 3. Comparison of basal and hFSH-stimulated cAMP as a function of receptor density for the WT and constitutively active hFSHR mutants. Basal (solid line) and hFSH-stimulated (dashed line) cAMP concentrations for each hFSHR construct are plotted together to more readily discern the hormonal responsiveness of each receptor. The data shown are taken from Fig. 2 and depict the mean \pm S.E. of triplicate determinations within one representative experiment. Similar results were obtained in three or more independent experiments.

I545^(5.46)L, and T580^(6.43)I). From Fig. 2A, it can be concluded that the hFSHR CAMs with the greatest basal constitutive activities are L460^(3.43)R and I545^(5.46)L. hFSHR(T580^(6.43)I) and hFSHR(M401^(2.43)T) exhibit moderate constitutive activity, whereas hFSHR(T449^(3.32)I) displays a very low level of constitutive activity.

The hormone responsiveness of each hFSHR CAM was also examined within the same experiment. The results, plotted for all of the hFSHR CAMs as compared with the WT hFSHR, are shown in Fig. 2B. Depicted this way, one can see that the two hFSHR CAMs with similarly moderate levels of constitutive activity, M401^(2.43)T and T580^(6.43)I, showed differing responses to hFSH. Whereas hFSHR(T580^(6.43)I) responds as well as, or even better than, the WT hFSHR to hFSH, the hormonal response of hFSHR(M401^(2.43)T) is less than that of the WT hFSHR. hFSHR T449^(3.32)I and L460^(3.43)R further exemplify the fact that the constitutive activities of the hFSHR CAMs do not necessarily correlate with their hormonal responsiveness. Whereas hFSHR(T449^(3.32)I) shows very little constitutive activity and hFSHR(L460^(3.43)R) exhibits high constitutive activity, both mutants produce lower concentrations of FSH-stimulated cAMP as compared with the WT hFSHR. The

other way to analyze the hormone responsiveness of the hFSHR CAMs is to compare the basal and hFSH-stimulated cAMP over varying receptor densities for each receptor construct. The results of these analyses are shown in Fig. 3. These graphs demonstrate that although the absolute concentrations of hFSH-stimulated cAMP in cells expressing hFSHR(T499^(3.32)I) or hFSHR(L460^(3.43)R) are similar, this reflects a robust hormone response by the T449^(3.32)I mutant but a very weak response by the L460^(3.43)R mutant. The high degree of constitutive activity and minimal hormonal responsiveness of the hFSHR(L460^(3.43)R) mutant are consistent with previously published data (26). With the exception of hFSHR(L460^(3.43)R), the hFSHR CAMs all showed a further increase in cAMP in response to hormone, although the responses varied quantitatively.

Basal and hCG-stimulated Activities of Cognate hLHR Mutants—We examined the basal and hCG-stimulated activities of the corresponding hLHR CAMs M398^(2.43)T, L457^(3.43)R, I542^(5.46)L, and T577^(6.43)I along with hLHR(T446^(3.32)I), which is the hLHR equivalent of the naturally occurring CAM hFSHR(T449^(3.32)I) (17). As shown in Fig. 4A, hLHR(T446^(3.32)I) exhibited little or no constitutive activity. In contrast, and as expected, the other hLHR mutants, known to be naturally occurring CAMs (34–37), displayed robust constitutive activities. Of the four hLHR CAMs examined, I542^(5.46)L displayed the greatest constitutive activity. Consistent with previously reported data (14), the basal activity of hLHR(L457^(3.43)R) does not show a linear relationship over a range of receptor concentrations. Therefore, although the constitutive activity of this mutant is greater than M398^(2.43)T and T577^(6.43)I at low receptor densities, its constitutive activity levels off as receptor densities are further increased, whereas those of M398^(2.43)T and T577^(6.43)I continue to increase.

The absolute concentrations of cAMP produced in response to a saturating concentration of hCG by the hLHR mutants compared with the WT hLHR are shown in Fig. 4B. hLHR(M398^(2.43)T) and hLHR(T577^(6.43)I) produced markedly higher concentrations of cAMP than the WT hLHR over the full range of receptor concentrations. It can also be seen that the concentrations of hCG-stimulated cAMP in cells expressing T446^(3.32)I were just slightly below those in cells expressing WT hLHR, whereas concentrations in cells expressing L457^(3.43)R

Activating Mutations of the hFSHR

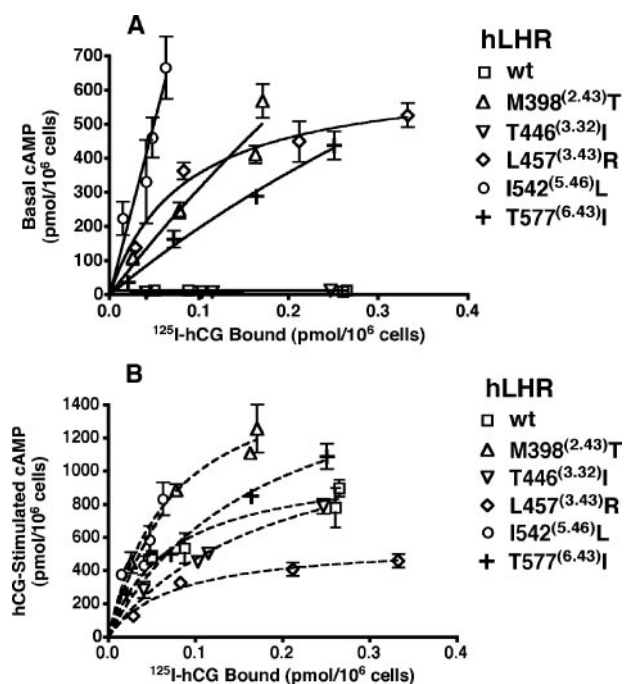


FIGURE 4. Basal and hCG-stimulated cAMP in corresponding hLHR activating mutants. HEK293 cells were transiently transfected with increasing amounts of plasmid encoding the indicated WT or mutant hLHRs. Plasmid concentrations were kept constant by the addition of empty vector pcDNA3.1(neo). In the same experiment, cell surface receptors, as measured by ^{125}I -hCG binding assays to intact cells, and cAMP measurements were performed. cAMP levels were determined under basal conditions (A) or after stimulation with hCG (100 ng/ml final concentration) (B). The data shown are from one representative experiment and depict the mean \pm S.E. of triplicate determinations within that experiment after subtracting the cAMP measured in cells expressing empty vector only. Similar results were obtained in three or more independent experiments.

were markedly lower than WT hLHR. As shown in Fig. 5, where the basal and hCG-stimulated cAMP concentrations produced by each hLHR construct are plotted relative to each other, the hLHR CAMs L457^(3.43)R and I542^(5.46)L do not show any increase in hCG-stimulated cAMP production over that already synthesized as a result of constitutive activity. Not all hLHR CAMs are unresponsive to hormone, however, as exemplified by M398^(2.43)T and T577^(6.43)I. Both of these CAMs cause an increase in hCG-stimulated cAMP above those levels synthesized as a result of constitutive activity. As would be expected, the hLHR mutant T446^(3.32)I, which is not constitutively active, shows a hormonal responsiveness similar to that of the WT hLHR.

Comparison of the hFSHR Versus hLHR Containing Homologous Substitutions—In the next set of experiments, we directly compared the basal activities of the WT hLHR and hFSHR and homologous mutations introduced into each receptor. The WT and M^(2.43)T, T^(3.32)I, and L^(3.43)R receptors were examined within one experiment (Experiment I), and the WT and I^(5.46)L and T^(6.43)I mutants were examined within another (Experiment II). Looking at Fig. 6, A and E, an expansion of the y axes permits one to observe that the WT hLHR exhibits a higher degree of basal constitutive activity than the WT hFSHR. In examining the activities of the mutants, the hLHR versions of M^(2.43)T (B), I^(5.46)L (F), and T^(6.43)I (G) all display constitutive activities \sim 10-fold higher

than their respective hFSHR counterparts. The hLHR mutant containing the L^(3.43)R substitution also showed greater constitutive activity than its hFSHR counterpart (D). However, because the constitutive activity of hFSHR(L460^(3.43)R) is much higher than the other hFSHR mutants and because the constitutive activity of hLHR(L457^(3.43)R) levels off at high receptor densities, the difference in activities of the L^(3.43)R mutation in the hLHR versus hFSHR is not as great. Of those mutations examined, the only case where the constitutive activity of a hFSHR mutant is greater than that of a hLHR mutant is that of T^(3.32)I (C), a naturally occurring hFSHR CAM (17). Whereas hLHR(T446^(3.32)I) shows no detectable constitutive activity, hFSHR(T449^(3.32)I) is, as previously reported (17), constitutively active. Nonetheless, the constitutive activity of hFSHR(T449^(3.32)I), like the other hFSHR CAMs, is extremely low as compared with the hLHR CAMs (note the expanded y axis in C).

Promiscuous Activation of hFSHR Versus hLHR CAMs—We next sought to determine if the hFSHR CAMs M401^(2.43)T, L460^(3.43)R, I545^(5.46)L, and T580^(6.43)I exhibit promiscuous activation by supramaximal concentrations of the related glycoprotein hormones hCG and hTSH, as has been reported for the naturally occurring hFSHR(T449^(3.34)I) (17) and the few other FSHR CAMs associated with OHSS in naturally conceived pregnancies (18–20) (Fig. 7). As with all the previous experiments shown, this experiment was performed using highly purified preparations of recombinant hormones. Cells were transiently transfected with predetermined amounts of plasmid that would yield cells expressing similar levels of cell surface receptor. At the concentrations of hormones used, the WT hFSHR exhibited a strong response to hFSHR and a very small, but statistically significant, response to high concentrations of hCG or hTSH. Consistent with previously published reports (17, 38), cells expressing hFSHR(T449^(3.32)I) responded robustly to supramaximal concentrations of hCG and hTSH. The four other hFSHR mutants, M401^(2.43)T, L460^(3.43)R, I545^(5.46)L, and T580^(6.43)I, which we determined from this study to be constitutively active, also exhibited strong responses to supramaximal concentrations of hCG and hTSH. The small responses of the WT hFSHR and the stronger responses of the hFSHR CAMs to high concentrations of hCG and TSH are specific, since no responses were observed in cells transfected with empty pcDNA3.1 as a control.

The cognate hLHR mutants were also examined for their ability to respond to supramaximal concentrations of hFSH or hTSH (Fig. 8). In this experiment, we chose not to decrease the expression of all of the other hLHR mutants to the low levels of expression of the I542^(5.46)L and M398^(2.43)T mutants. Therefore, although the expression of the WT, T446^(3.32)I, L457^(3.43)R, and T577^(6.43)I hLHRs are similar, they are higher than those of I542^(5.46)L and M398^(2.43)T, and this should be taken into account when comparing the basal or hormone-stimulated activities between the different hLHR constructs. The WT hLHR responded robustly to hCG but exhibited little or no response to supramaximal concentrations of hFSH or hTSH. The hLHR mutant T446^(3.32)I, which exhibits little or no constitutive activity, behaved similarly to the WT hLHR. Of

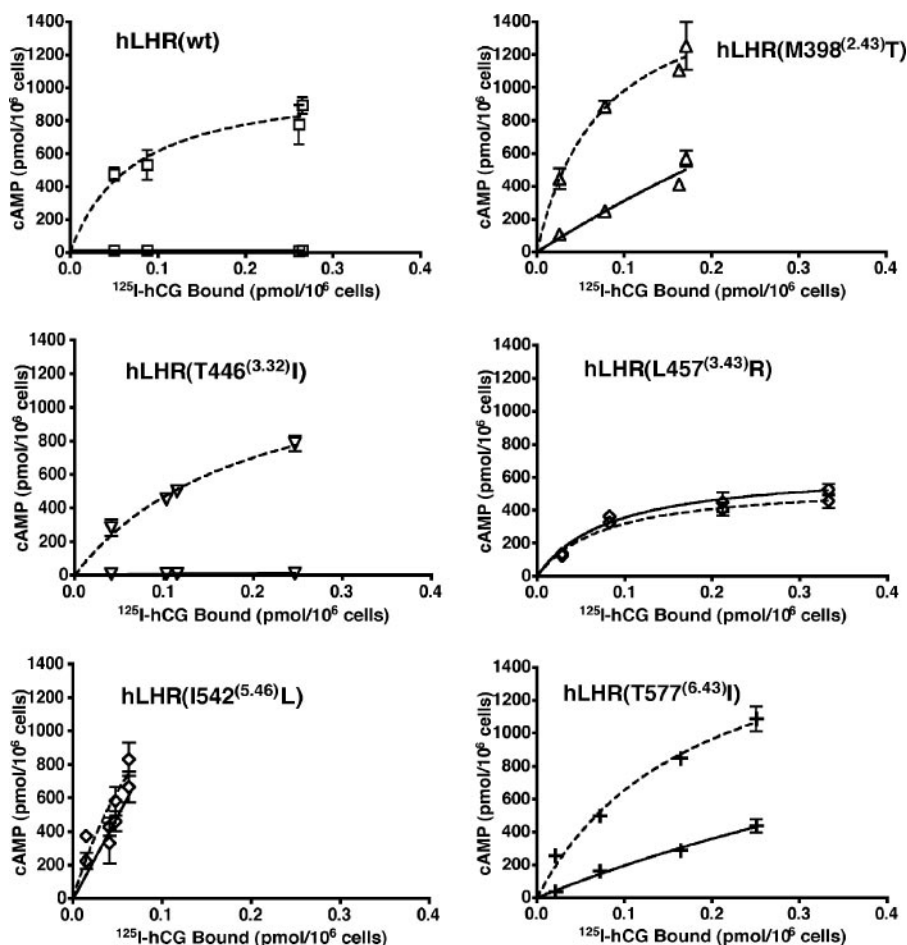


FIGURE 5. Comparison of basal and hCG-stimulated cAMP as a function of receptor density for the WT and constitutively active hLHR mutants. Basal (solid line) and hCG-stimulated (dashed line) cAMP concentrations for each hLHR construct are plotted together to more readily discern the hormonal responsiveness of each receptor. The data shown are taken from Fig. 4 and depict the mean \pm S.E. of triplicate determinations within that experiment after subtracting the cAMP measured in cells expressing empty vector only. Similar results were obtained in three or more independent experiments.

those hLHR mutants that are distinctly constitutively active, M398^(2.43)T, I542^(5.46)L, and T577^(6.43)I responded to hCG as would be expected. These hLHR CAMs also exhibited very small increases in cAMP in response to high concentrations of hFSHR and hTSH. Which of these small increases reached statistical significance varied between experiments. Cells transfected with empty vector did not respond to the same concentrations of hFSH or hTSH. The L457^(3.43)R mutant, which shows little to no response to hCG despite normal hCG binding affinity (39), similarly displayed little or no response to high concentrations of hFSH or hTSH.

Computational Modeling of the hFSHR—In this study, the same computational approach previously employed to investigate mutation-induced active states of the hLHR has been applied to the hFSHR. Comparative analyses of the structures averaged over all of the 2000 frames constituting each 1 ns trajectory focused on the triggers of the constitutive activity of M401^(2.43)T, L460^(3.43)R, I545^(5.54)L, and T580^(6.43)I as well as on the structural features that differentiate these active hFSHR mutants from the WT hFSHR. Mutation of Met-401^(2.43) to threonine induces a reduction in the van der Waals interactions found in the WT hFSHR between the native methionine and

Tyr-626^(7.53) of the NPXXY highly conserved motif. Furthermore, loss of van der Waals interactions at this mutation site is associated with the gain of a weak hydrogen bond between Thr^(2.43) and Arg^(6.36). As for the hFSHR(L460^(3.43)R) mutant, the trigger of constitutive activity seems to be the formation of a charge-reinforced hydrogen bond between the replacing arginine and Asp-581^(6.44). Arg-460^(3.43) performs additional hydrogen bonds with the conserved Asn-618^(7.45) and Asn-622^(7.49). Finally, changes in interhelical van der Waals interactions characterize both the I545^(5.54)L and T580^(6.43)I hFSHR CAMs. The former mutation is located at the interface between H3 and H6 and interacts with the activating mutation site Leu-460^(3.43), whereas T580^(6.43)I is adjacent to Asp-581^(6.44) at the interface between H6 and H7.

The activating mutations of the hFSHR induce a weakening of the salt bridge interactions found in the WT receptor between Arg-467^(3.50) of the (E/D)R(Y/W) highly conserved motif and either the adjacent Glu-466^(3.49) or Asp-567^(6.30). The most effective hFSHR CAM in this respect appears to be the L460^(3.43)R mutant that is characterized by the complete loss of the

Arg^(3.50)-Asp^(6.30) interaction (Fig. 9). A feature common to all of the hFSHR CAMs is the increase, with respect to the WT receptor, in the solvent-accessible surface area (SAS) of selected amino acids at the cytosolic interface between H3, H5, and H6 (Fig. 9). Two SAS indices made of the contribution of different amino acids (*i.e.* SAS₁ and SAS₂) appeared to correlate with the functional receptor state (*i.e.* nonactive or active). In detail, SAS₁ was computed over Arg-467^(3.50), Ile-471^(3.54), Thr-555, and Val-556 (both in IL3) (*i.e.* SAS₁), and it was 51, 82, 80, 139, and 77 Å² in the WT hFSHR, M401^(2.43)T, L460^(3.43)R, I545^(5.46)L, and T580^(6.43)I, respectively. The alternative index, SAS₂, computed on the same amino acids as SAS₁ with the addition of Arg-398^(2.40) and Asp-567^(6.30), was 156, 175, 190, 211, and 227 Å² for the WT hFSHR, M401^(2.43)T, T580^(6.43)I, I545^(5.46)L, and L460^(3.43)R, respectively.

DISCUSSION

Previous reports have shown that the introduction of the activating D^(6.44)G mutation of the hLHR into the structurally related hFSHR does not cause constitutive activity (24, 25). These observations prompted the proposal that the hFSHR may be more resistant to mutation-induced constitutive activa-

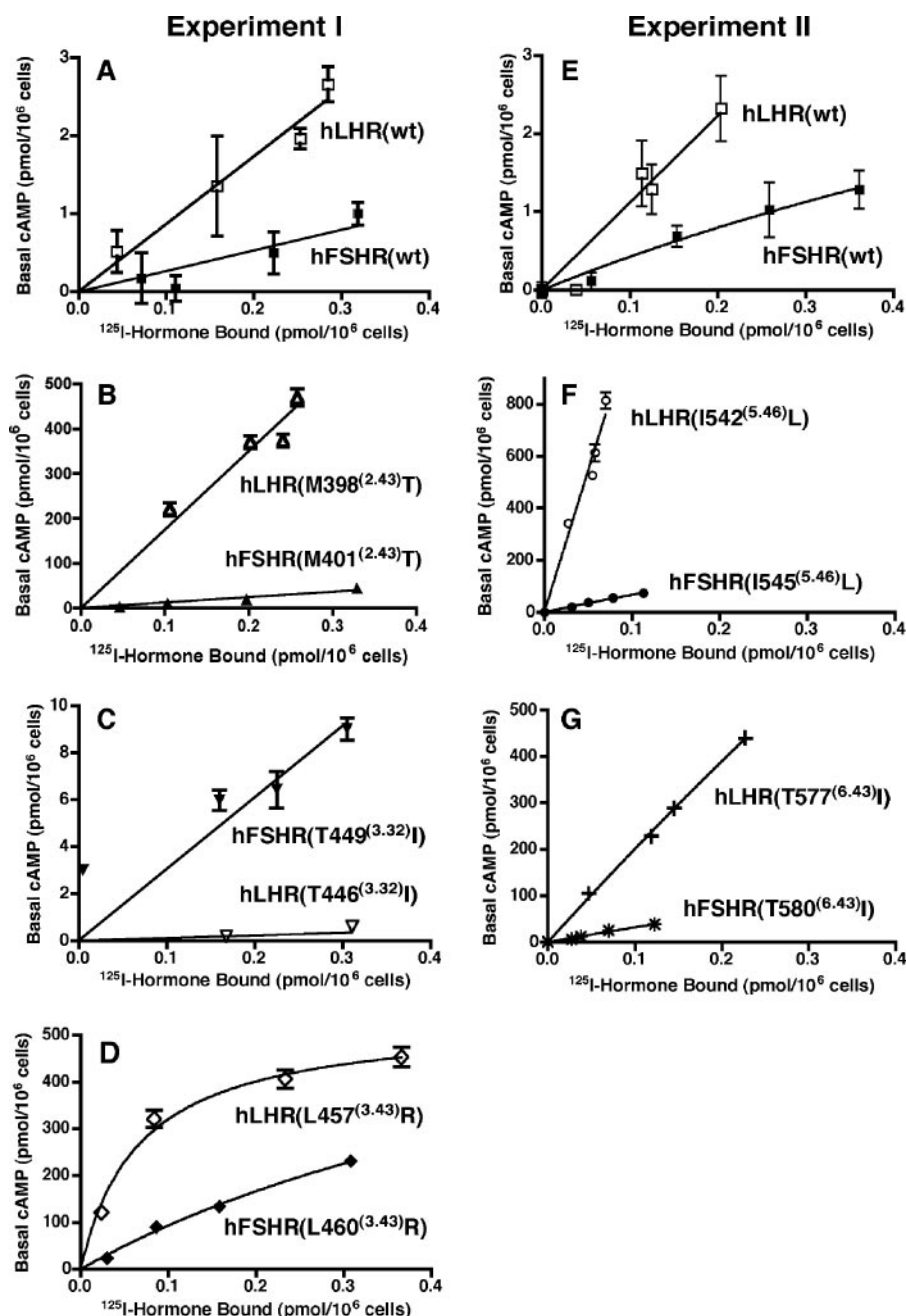


FIGURE 6. Comparison of the degree of constitutive activity for a given mutation in the hLHR as compared with the hFSHR. HEK293 cells were transiently transfected with increasing concentrations of the WT hLHR, WT hFSHR, or indicated mutants thereof. Plasmid concentrations were kept constant by the addition of empty vector pcDNA3.1(neo). In the same experiment, cell surface receptor number, as measured by ^{125}I -hCG (for the hLHR) or ^{125}I -hFSHR (for the hFSHR) binding assays to intact cells, and basal cAMP determinations were performed. Binding data are expressed as pmol of hormone bound/ 10^6 cells, thus correcting for differences in the molecular weights of hFSH and hCG. *Open symbols* depict results for the hLHR, *closed symbols* for the hFSHR. The data in the *leftmost panels* were determined from one experiment, and those in the *rightmost panels* are from a separate experiment. Both experiments were replicated at least three times with similar results. The data shown are from one representative experiment and depict the mean \pm S.E. of triplicate determinations within that experiment after having subtracting the cAMP measured in cells expressing empty vector only. Note that the *scales* of the *y axes* are different.

tion than the hLHR. However, another report showed that the hLHR-activating mutation L^(3.43)R, when introduced into the hFSHR, resulted in strong hFSHR constitutive activation (26) and indicated that the hFSHR was not totally resistant to mutation-induced constitutive activation. Consistent with this, five different naturally occurring activating mutations of the hFSHR have been identified (16–20). Because a direct compar-

ison of the activities of the hLHR and hFSHR containing the same mutations had not been done for many mutations over different regions of the receptors, the question remained unanswered, however, as to whether or not the hFSHR was generally more resistant to mutation-induced constitutive activity than the hLHR. This question is of physiological relevance because the number of naturally occurring activating mutations of the hFSHR that have been identified is much smaller than those described for the hLHR.

The data presented show that the hFSHR is indeed generally much less susceptible to mutation-induced constitutive activity as compared with the hLHR containing the same mutations. Even with the WT receptors, the WT hLHR possesses a greater basal constitutive activity than the hFSHR when compared over a similar range of cell surface receptor densities. An even more pronounced difference is observed between these two gonadotropin receptors when comparing the constitutive activities of homologous mutations introduced into each of them. Of nine mutations known to cause constitutive activation of the hLHR, we identified three corresponding hFSHR mutations, M401^(2.43)T, I545^(5.46)L, and T580^(6.43)I, that appear in this study to have the greatest activity (~3-fold greater activity than the WT hFSHR). We had previously shown (26), and confirm herein, that the introduction of the hLHR-activating mutation L^(3.43)R into the hFSHR also causes constitutive activation of the hFSHR. We also compared the activities of the hLHR and hFSHR CAMs containing the M^(2.43)T, I^(5.46)L, T^(6.43)I, and L^(3.43)R mutations. In all these

cases, the hFSHR CAM exhibited much lower constitutive activity than the cognate hLHR CAM.

Several years ago, one naturally occurring mutation of the hFSHR, D567^(6.30)G, was identified in a hypophysectomized man who exhibited autonomous spermatogenesis (16). However, it has not always been possible to demonstrate the constitutive activity of this hFSHR mutant *in vitro* (24).⁶ More

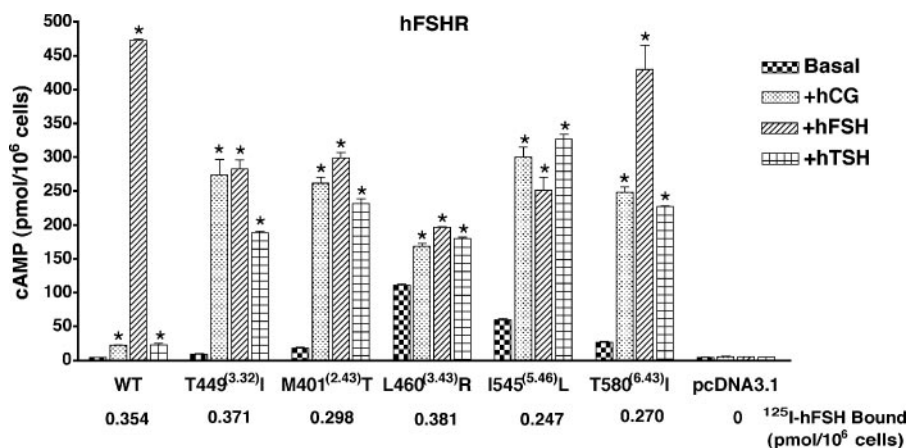


FIGURE 7. Promiscuous activation of hFSHR constitutively active mutants. HEK293 cells were transiently transfected with the WT hFSHR or constitutively active hFSHR mutants to yield similar levels of cell surface receptor expression. In the same experiment, cells were assayed for ^{125}I -FSH binding and for cAMP levels determined after incubation with no additions (*Basal*), a supramaximal concentration of hCG (100 IU/ml), a maximal concentration of hFSH (10 IU/ml), or a supramaximal concentration of hTSH (100 mIU/ml). The data shown are the mean \pm S.E. of triplicate determination from a single experiment representative of two independent experiments. The asterisks denote the hormone-stimulated cAMP concentrations that are statistically different ($p < 0.05$) from the basal concentration of cAMP measured in cells transfected with the same construct.

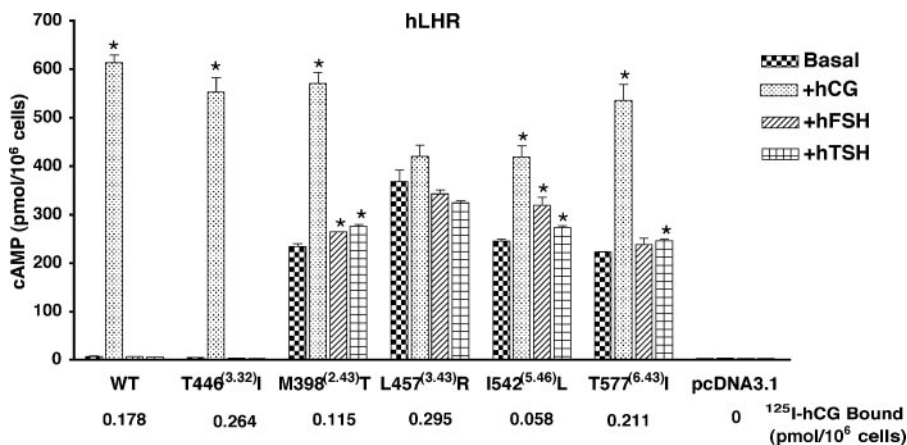


FIGURE 8. Lack of promiscuous activation of hLHR constitutively active mutants. HEK293 cells were transiently transfected with the WT hLHR or constitutively active hLHR mutants to yield similar levels of cell surface receptor expression. In the same experiment, cells were assayed for ^{125}I -hCG binding and for cAMP levels determined after incubation with no additions (*Basal*), a maximal concentration of hCG (1 IU/ml), a supramaximal concentration of hFSH (100 IU/ml), or a supramaximal concentration of hTSH (30 mIU/ml). The data shown are the mean \pm S.E. of triplicate determination from a single experiment representative of two independent experiments. The asterisks denote the hormone-stimulated cAMP concentrations that are statistically different ($p < 0.05$) from the basal concentration of cAMP measured in cells transfected with the same construct.

recently, four different mutations of the hFSHR, T449^(3.32)I (17), D567^(6.30)N (18), T449^(3.32)A (19), and I545^(5.54)T (20), have been identified in women with OHSS resulting from the promiscuous stimulation of the hFSHR by normally elevated levels of hCG during naturally conceived pregnancy. Interestingly, T449^(3.32)I, T449^(3.32)A, and I545^(5.54)T were also reported to exhibit constitutive activity, although there did not appear to be any pathophysiological consequences observed in the women outside of pregnancy due to hFSHR constitutive activation (18–20). A subsequent report by Montanelli *et al.* (38) further characterizing the properties of these hFSHR mutants described constitutive activity for the T449^(3.32)I mutant.

The data presented herein confirm the constitutive nature of hFSHR(T449^(3.32)I). We also show that the homologous T^(3.32)I

substitution made in the hLHR causes little or no detectable constitutive activity. It is possible, therefore, that the lower constitutive activities we observed when hFSHR CAMs were produced by introducing known hLHR activating mutations may simply be due to the fact that the derivative mutation is not as active as that in the parent receptor. However, regardless of whether the hFSHR CAM is a naturally occurring mutation or is a derivative of a naturally occurring hLHR CAM, the constitutive activities of all of the hFSHR CAMs examined are consistently markedly lower than the hLHR CAMs. For example, in Fig. 6, where the activities of cognate hLHR and hFSHR CAMs are shown, at a cell surface receptor level of 0.1 pmol of hormone bound/10⁶ cells, the basal cAMP levels of the hLHR CAMs are ~200–800 pmol/10⁶ cells, whereas the basal cAMP levels of the hFSHR CAMs at the same receptor density are ~3–80 pmol/10⁶ cells. Taken together, these data show that, for a variety of mutations over different regions of the receptors and originating as naturally occurring mutations of either the hLHR or hFSHR, the hFSHR is indeed generally more refractory to mutation-induced constitutive activation than the hLHR. It is possible, therefore, that some of the conflicting data regarding the presence or absence of constitutive activity of some hFSHR mutants (*i.e.* D567^(6.30)G and T449^(3.32)I) may be due to the inherent difficulties in detecting such low levels of constitutive activity.

In contrast to the hLHR, in which numerous activating mutations have been associated with gonadotropin-independent precocious puberty in boys (as reviewed in Refs. 5 and 6), and the other glycoprotein hormone receptor, hTSHR, in which many activating mutations have been identified associated with a hyperthyroidism and thyroid adenomas (as reviewed in Ref. 40), there is only one instance where a hFSHR mutation has been identified based on its constitutive activity *in vivo* (16). This mutation, as discussed above, was identified in the very isolated context of a hypophysectomized man (16). Based upon our results, we suggest that even if unidentified activating mutations occur in the hFSHR gene at the same frequency as in the hLHR and hTSHR genes, resulting physiological abnormalities are far less likely

Activating Mutations of the hFSHR

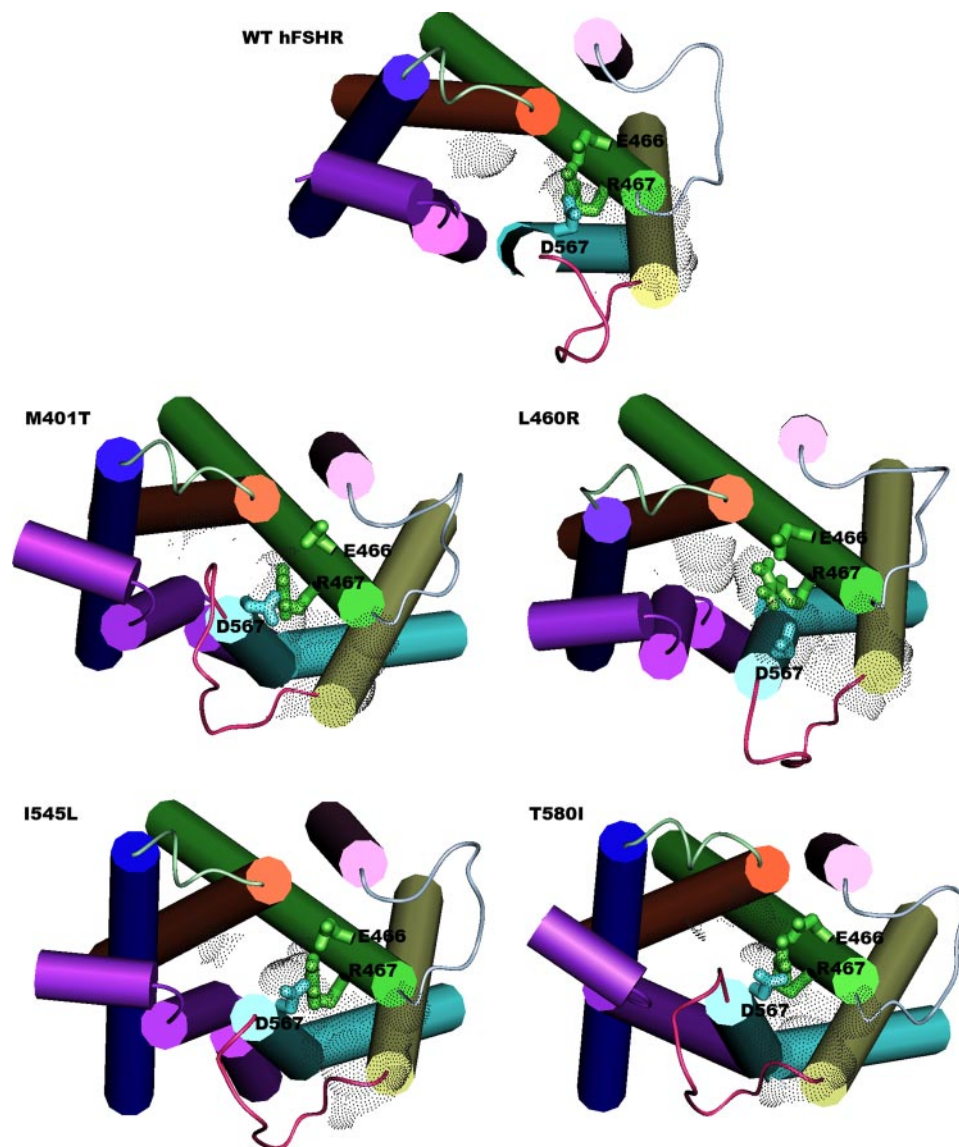


FIGURE 9. Computational models of the WT hFSHR and CAMs. Shown are top views from the intracellular side of the WT hFSHR and the M401^(2,43)T, T580^(6,43)I, I545^(5,46)L, and L460^(3,43)R hFSHR CAMs. Helices 1, 2, 3, 4, 5, 6, and 7 are colored in blue, orange, green, pink, yellow, cyan, and violet, respectively. Helix 8 is colored in violet as well. The intracellular loops 1, 2, and 3 are colored in light green, gray, and purple, respectively. The side chains of Glu-466^(3,49), Arg-467^(3,50), and Asp-567^(6,30) are shown in a stick representation and colored according to their location. The SAS computed over Arg-398^(2,40), Arg-467^(3,50), Ile-471^(3,54), Thr-555, and Val-556 (both in IL3) and Asp-567^(6,30) (*i.e.* SAS₂) is also shown, represented by gray dots. SAS₁ values are 156, 175, 190, 211, and 227 Å² for the WT hFSHR and the M401^(2,43)T, T580^(6,43)I, I545^(5,46)L, and L460^(3,43)R hFSHR CAMs, respectively.

to be observed due to the extremely low levels of constitutive activity of hFSHR CAMs.

At physiological concentrations of hormones, the glycoprotein hormone receptors appear exquisitely selective, responding uniquely to the appropriate hormone. However, it has been shown and is confirmed herein that at exceptionally high concentrations, the inappropriate hormone (even highly purified recombinant hormone) can elicit a small but measurable response in the WT hFSHR (19, 20, 41). Furthermore, in OHSS, the mutations that cause the hFSHR to be constitutively active also cause them to become more sensitive to supramaximal concentrations of hCG and hTSH (17–20), where the inappropriate response to high concentrations of hCG secreted during pregnancy causes excessive ovarian stimulation. The results

presented here on hCG and hTSH stimulation of the laboratory-designed hFSHR CAMs lend further support to the tenet that promiscuous activation of the hFSHR mutant accompanies its constitutive activation. As has been previously reported for the naturally occurring hFSHR CAMs associated with OHSS (17–20), specific ¹²⁵I-hCG binding was not observed for any of the hFSHR CAMs in the present study. Therefore, whether the activating hFSHR mutations have no effect on hCG binding affinity or if they increase hCG binding affinity, but this increased affinity remains below detection levels, cannot be determined.

Previous studies have reported that, in contrast to hFSHR CAMs, hTSHR CAMs do not exhibit promiscuous activation (38). From these data alone, however, it could not be determined if promiscuous activation resulting from mutation-induced constitutive activation was restricted to the hFSHR or if this was a property of both gonadotropin receptors. We show herein that hLHR CAMs respond, albeit very weakly, to supramaximal concentrations of hFSH and hTSH. A comparison of the -fold stimulations above basal level of the hFSHR and hLHR CAMs (compare Figs. 7 and 8), however, clearly shows that the promiscuous activation of hFSHR CAMs is far greater than that of hLHR CAMs. Therefore, our data show that the hFSHR is unique among the glycoprotein hormone receptors in that basal, as well as mutation-induced, constitutive activities of the hFSHR are much lower than the other receptors, and only hFSHR CAMs display strong promiscuous activation.

Previous computational modeling of WT and mutated hLHRs provided insights into the structural hallmarks of mutation-induced active and inactive forms of the hLHR. In this respect, a common and peculiar feature of all of the CAMs that is not shared with the WT hLHR was the opening of a cytosolic crevice between IL2 and IL3 and between H3 and H6 (12–14, 39, 42). This structural effect was properly accounted for by the SAS computed over selected amino acids, including the (E/D)R(Y/W) arginine (*i.e.* Arg-464^(3,50), Thr-467^(3,53), Ile-468^(3,54), and Lys-563^(6,29)). The composite SAS index proved to be an effective hallmark of the functional hLHR state,

being $<50 \text{ \AA}^2$ in the WT and inactive forms and $>50 \text{ \AA}^2$ in the active forms (12, 13). The SAS index was successfully probed in its ability to predict the functional behavior (*i.e.* active and non-active) of a number of artificial mutants of the hLHR (12–14). Another feature of the most active hLHR mutants, as inferred from the latest computational analyses, was the weakening of either one or both of the charge-reinforced hydrogen bonding interactions found in the WT hLHR between Arg-464^(3.50) of the (E/D)R(Y/W) motif and both Glu-463^(3.49) and Asp-564^(6.30). These results strengthen the hypothesis that both of these coulombic interactions involving the (E/D)R(Y/W) arginine, inherited from the rhodopsin structure, contribute to maintaining the inactive state of the hLHR. Changes in the SAS index were, however, the best hallmarks of the absence or presence of constitutive activity.

The extensive *in silico* mutagenesis experiments on naturally occurring as well as artificial single and multiple activating mutations of the hLHR made it possible to infer the structural triggers of mutation-induced receptor activation (15). Two of these mutations (*i.e.* M^(2.43)T and L^(3.43)R) have also been found to induce constitutive activity in the hFSHR (as shown here and, for L^(3.43)R, also in Ref. 26). In the hLHR, the trigger of the activation by Met-398^(2.43) mutations was suggested to be size reduction of the replacing side chain (13). This effect is associated with reduction in the strength of the interaction between the replacing amino acid and the highly conserved tyrosine of the (E/D)R(Y/W) motif. In contrast to Met-398^(2.43), only cationic amino acid substitutions for Leu-457^(3.43) resulted in constitutive activity (14, 39). Computational modeling suggested that, in this case, the activation trigger is a salt bridge between positions 3.43 and 6.44. In the hLHR(L457^(3.43)R) mutant, the formation of such an interhelical salt bridge is allowed by the presence of Asp-578^(6.44) in the proximity to the mutated position.

This study highlights commonalities and differences between the computational models of the WT and CAM forms of the hFSHR and hLHR. Similar to the hLHR, the mutation of Met-401^(2.43) to threonine in the hFSHR induces a reduction in the van der Waals interactions found in the WT receptor between the native methionine and Tyr-626^(7.53) of the NPXXY highly conserved motif. In contrast to the hLHR, the loss of van der Waals interactions at this mutation site is associated with the gain of a weak hydrogen bond between Thr^(2.43) and Arg^(6.36). Such an interaction could not be observed in the corresponding mutant of the hLHR, in which a lysine substitutes for Arg^(6.36). This structural difference could correlate, at least in part, with the significantly lower constitutive activity of hFSHR(M401^(2.43)T) compared with hLHR(M398^(2.43)T). In contrast, remarkable structural similarities between the hFSHR and hLHR are apparent with the strongest hFSHR CAM (*i.e.* L460^(3.43)R). In fact, similar to the hLHR (14), the trigger of constitutive activity in this hFSHR mutant seems to be the formation of a charge-reinforced hydrogen bond between the replacing arginine and Asp-581^(6.44). Arg-460^(3.43) performs additional hydrogen bonds with the conserved Asn-618^(7.45) and Asn-622^(7.49). Finally, changes in interhelical van der Waals interactions characterize both the I545^(5.54)L and T580^(6.43)I hFSHR CAMs. The latter, which is adjacent to the Asp-581^(6.44)

CAM site, lies at the interface between H6 and H7. Two positions at this interface and in the proximity to the 580^(6.43) CAM site (*i.e.* 6.39 and 7.42) hold different amino acids in the hFSHR and the hLHR. Indeed, position 6.39 holds a methionine in the hFSHR and a threonine in the hLHR, whereas position 7.42 holds a histidine in the hFSHR and a tyrosine in the hLHR. Amino acid differences at 7.42 appear to influence the interaction pattern of Asp^(6.44). In fact, in the WT hLHR, Tyr^(7.42) may be found interacting with Asp^(6.44), whereas, in the WT hFSHR, the corresponding His^(7.42), which has been simulated in its neutral state, does not. These differences could implicate different structural/functional responses of the two receptors to mutations at the middle portion of the H6-H7 interface. Further support for this hypothesis comes from earlier studies comparing the D^(6.44)G mutation in the human *versus* rat FSHRs. Although this mutation induces constitutive activity in the rat FSHR, it is without effect in the hFSHR (25). Interestingly, residues 6.39 and 7.42 (threonine and tyrosine in the rat FSHR; methionine and histidine in the hFSHR) were shown to play key roles in permitting or suppressing constitutive activity by the D^(6.44)G mutation (25).

Similar to the hLHR, the activating mutations of the hFSHR tend to weaken the salt bridge interactions found in the WT receptor between Arg-467^(3.50) of the (E/D)R(Y/W) highly conserved motif and either the adjacent Glu-466^(3.49) or Asp-567^(6.30). The most effective hFSHR CAM in this respect appears to be the L460^(3.43)R mutant that is characterized by the complete loss of the Arg^(3.50)–Asp^(6.30) interaction (Fig. 9). Similar to the hLHR, changes in the interaction patterns of Arg^(3.50) are, however, less effective as hallmarks of the functional receptor state (*i.e.* nonactive or active) than changes in the solvent accessibility of selected amino acids in the cytosolic domains. Indeed, similar to the hLHR, a feature common to all of the hFSHR CAMs is the increase (with respect to the WT receptor) in the solvent accessibility of selected amino acids at the cytosolic interface between H3, H5, and H6 (Fig. 9). This effect is properly marked by the SAS₁ and SAS₂ indices, which differ from each other with respect to the amino acids employed in SAS computation (*i.e.* two more amino acids, Arg-398^(2.40) and Asp-567^(6.30), contribute to the SAS₂ index compared with SAS₁). In detail, the SAS₁ indices of the lowest (M401^(2.43)T) and highest (L460^(3.43)R) hFSHR active mutants are 31 and 29 \AA^2 higher than that of the WT hFSHR. In contrast, the SAS₂ indices of the lowest and highest active mutants are 19 and 71 \AA^2 higher than that of the WT receptor. The good correlation between the SAS₂ index and basal activity values also holds for the other simulated hFSHR mutants. Collectively, the SAS₂ is 156, 175, 190, 211, and 227 \AA^2 for the WT hFSHR, M401^(2.43)T, T580^(6.43)I, I545^(5.46)L, and L460^(3.43)R, respectively, consistent with the fact that the basal activity rank order is WT < M401^(2.43)T < T580^(6.43)I < I545^(5.46)L < L460^(3.43)R. This trend supports the inference that an augmentation in solvent exposure, with respect to the WT receptor, in selected portions of the cytosolic domains is the most relevant structural feature shared in common by the active mutants of the hFSHR. Thus, the different CAMs of the same receptor (*i.e.* hLHR or hFSHR) or the homologous CAMs in the two gona-

Activating Mutations of the hFSHR

dotropin receptors, although structurally different, share an augmentation in solvent exposure, as compared with the WT, of selected cytosolic amino acids in the cytosolic extensions of H3, H5, and H6. Such an increase in solvent exposure is not associated with significant reciprocal movements of H3 and H6 as predicted by early biophysical studies on rhodopsin photoactivation (43). Our results are in striking agreement with the very recently released structure of a photoactivated deprotonated rhodopsin intermediate, reminiscent of MII, at 4.15 Å resolution (44). Indeed, comparisons of the low resolution structures of dark and photoactivated rhodopsin reveal that the changes that accompany photoactivation are smaller than previously predicted for MII (44). Interestingly, consistent with the results of computational modeling of mutation-induced active and inactive states of the gonadotropin receptors, slight increases in the solvent accessibility of selected amino acids at the cytosolic surface of H3 and H6 appear to be the major relevant structural differences between the dark and the photoactivated states of rhodopsin (results not shown). Collectively, the structural commonalities between mutation-induced active states of the gonadotropin receptors and photoactivated states of rhodopsin would suggest that the increase in solvent accessibility at the cytosolic extension of H3, H5, and H6 is the major structural feature also differentiating the hormone-induced active states from the ground states of hFSHR and hLHR. In this respect, we postulate that mutation- and hormone-induced active states of the gonadotropin receptors, although fundamentally different, would share common structural differences from the inactive states, residing in the solvent accessibility of selected cytosolic amino acids in the environment of the (E/D)R(Y/W) highly conserved motif.

Collectively, the results of this study suggest that, similar to the hLHR, the target of the structural information transfer from the activating mutation sites in the hFSHR is the environment of the highly conserved arginine of the (E/D)R(Y/W) motif (*i.e.* the cytosolic extensions of H3, H5, and H6). The cytosolic amino acids that undergo an increase in solvent accessibility in going from the inactive to the active forms are, however, different in the two receptors, suggesting possible differences in the receptor-G protein interface, which may correlate with the different functional response of hFSHR compared with the hLHR. Clearly, further experiments are needed to explore this hypothesis.

In conclusion, computational experiments suggest that the mechanisms through which homologous mutations increase the basal activity of the hLHR and the hFSHR are very similar. This is particularly true for the strongest hFSHR CAMs like L460^(3,43)R and I545^(5,46)L. The demonstrated decreased susceptibility to constitutive activity of the hFSH compared with the hLHR and the greater promiscuous activity of hFSH CAMs compared with hLHR CAMs may, therefore, be due to differences in the shape and electrostatics features of the solvent-exposed cytosolic receptor domains involved in the receptor-G protein interface rather than to differences in the nature of the local perturbation at the mutation site or in the way such local perturbation is transferred to the putative G protein binding domains.

Acknowledgment—We thank Nathan Johnson for expert technical assistance.

REFERENCES

1. Ascoli, M., Fanelli, F., and Segaloff, D. L. (2002) *Endocr. Rev.* **23**, 141–174
2. Simoni, M., Gromoll, J., and Nieschlag, E. (1997) *Endocr. Rev.* **18**, 739–773
3. Hsu, S. Y., Kudo, M., Chen, T., Nakabayashi, K., Bhalla, A., van der Spek, P. J., van Duin, M., and Hsueh, A. J. (2000) *Mol. Endocrinol.* **14**, 1257–1271
4. Fan, Q. R., and Hendrickson, W. A. (2005) *Nature* **433**, 269–277
5. Latronico, A., and Segaloff, D. (1999) *Am. J. Hum. Genet.* **65**, 949–958
6. Themmen, A. P. N., and Huhtaniemi, I. T. (2000) *Endocr. Rev.* **21**, 551–583
7. Ballesteros, J. A., and Weinstein, H. (1995) *Methods Neurosci.* **25**, 366–428
8. Liu, G., Duranteau, L., Carel, J.-C., Monroe, J., Doyle, D. A., and Shenker, A. (1999) *N. Engl. J. Med.* **341**, 1731–1736
9. Richter-Unruh, A., Wessels, H. T., Menken, U., Bergmann, M., Schmittmann-Ohters, K., Schaper, J., Tappeser, S., and Hauffa, B. P. (2002) *J. Clin. Endocrinol. Metab.* **87**, 1052–1056
10. Hirakawa, T., Galet, C., and Ascoli, M. (2002) *Endocrinology* **143**, 1026–1035
11. Hirakawa, T., and Ascoli, M. (2003) *Endocrinology* **144**, 3872–3878
12. Angelova, K., Fanelli, F., and Puett, D. (2002) *J. Biol. Chem.* **277**, 32202–32213
13. Fanelli, F., Verhoef-Post, M., Timmerman, M., Zeilemaker, A., Martens, J. W., and Themmen, A. P. (2004) *Mol. Endocrinol.* **18**, 1499–1508
14. Zhang, M., Mizrachi, D., Fanelli, F., and Segaloff, D. L. (2005) *J. Biol. Chem.* **280**, 26169–26176
15. Fanelli, F., and De Benedetti, P. G. (2005) *Chem. Rev.* **105**, 3297–3351
16. Gromoll, J., Simoni, M., and Nieschlag, E. (1996) *J. Clin. Endocrinol. Metab.* **81**, 1367–1370
17. Vasseur, C., Rodien, P., Beau, I., Desroches, A., Gerard, C., de Poncheville, L., Chapel, S., Savagner, F., Croue, A., Mathieu, E., Lahlou, N., Descamps, P., and Misrahi, M. (2003) *N. Engl. J. Med.* **349**, 753–759
18. Smits, G., Olatunbosun, O., Delbaere, A., Pierson, R., Vassart, G., and Costagliola, S. (2003) *N. Engl. J. Med.* **349**, 760–766
19. Montanelli, L., Delbaere, A., Di Carlo, C., Nappi, C., Smits, G., Vassart, G., and Costagliola, S. (2004) *J. Clin. Endocrinol. Metab.* **89**, 1255–1258
20. De Leener, A., Montanelli, L., Van Durme, J., Chae, H., Smits, G., Vassart, G., and Costagliola, S. (2006) *J. Clin. Endocrinol. Metab.* **91**, 555–562
21. Fuller, P. J., Verity, K., Shen, Y., Mamers, P., Jobling, T., and Burger, H. G. (1998) *J. Clin. Endocrinol. Metab.* **83**, 274–279
22. Ligtenberg, M. J., Siers, M., Themmen, A. P., Hanselaar, T. G., Willemsen, W., and Brunner, H. G. (1999) *J. Clin. Endocrinol. Metab.* **84**, 2233–2234
23. Montgomery, G. W., Duffy, D. L., Hall, J., Kudo, M., Martin, N. G., and Hsueh, A. J. (2001) *Lancet* **357**, 773–774
24. Kudo, M., Osuga, Y., Kobilka, B. K., and Hsueh, A. J. W. (1996) *J. Biol. Chem.* **271**, 22470–22478
25. Tao, Y.-X., Mizrachi, D., and Segaloff, D. L. (2002) *Mol. Endocrinol.* **16**, 1881–1892
26. Tao, Y.-X., Abell, A. N., Liu, X., Nakamura, K., and Segaloff, D. L. (2000) *Mol. Endocrinol.* **14**, 1272–1282
27. Ho, S. N., Hunt, H. D., Horton, R. M., Pullen, J. K., and Pease, L. R. (1989) *Gene (Amst.)* **77**, 51–59
28. Horton, R. M., Hunt, H. D., Ho, S. N., Pullen, J. K., and Pease, L. R. (1989) *Gene (Amst.)* **77**, 61–68
29. Chen, C., and Okayama, H. (1987) *Mol. Cell. Biol.* **7**, 2745–2752
30. Sali, A., and Blundell, T. L. (1993) *J. Mol. Biol.* **234**, 779–815
31. Okada, T., Sugihara, M., Bondar, A. N., Elstner, M., Entel, P., and Buss, V. (2004) *J. Mol. Biol.* **342**, 571–583
32. MacKerell, A. D., Jr., Bashford, D., Bellott, R. L., Dunbrack, R. L., Jr., Evanseck, J. D., Field, M. J., Fisher, S., Gao, J., Guo, H., Ha, S., Joseph-McCarthy, D., Kuchnir, L., Kuczera, K., Lau, F. T. K., Mattos, C., Michnick, L., Ngo, T., Nguyen, D. T., Prodhom, B., Reiher, W. E., III, Roux,

- B., Schlendkrich, M., Smith, J. C., Stote, R., Straub, J., Watanabe, M., Wiorkiewicz-Kuczera, J., Yin, D., and Karplus, M. (1998) *J. Phys. Chem. B* **102**, 3586–3616
33. Im, W., Feig, M., and Brooks, C. L., III (2003) *Biophys. J.* **85**, 2900–2918
34. Yano, K., Kohn, L. D., Saji, M., Kataoka, N., Okuno, A., and Cutler, G. B., Jr. (1996) *Biochem. Biophys. Res. Commun.* **220**, 1036–1042
35. Latronico, A. C., Abell, A. N., Arnhold, I. J. P., Liu, X., Lins, T. S. S., Brito, V. N., Billerbeck, A. E., Segaloff, D. L., and Mendonca, B. B. (1998) *J. Clin. Endocrinol. Metab.* **83**, 2435–2440
36. Laue, L., Chan, W.-C., Hsueh, A., Kudo, M., Hsu, S. Y., Wu, S., Blomberg, L., and Cutler, G. B. (1995) *Proc. Natl. Acad. Sci. U. S. A.* **92**, 1906–1910
37. Kosugi, S., Van Dop, C., Geffner, M. E., Rabl, W., Carel, J. C., Chaussain, J. L., Mori, T., Merendino, J. J., Jr., and Shenker, A. (1995) *Hum. Mol. Genet.* **4**, 183–188
38. Montanelli, L., Van Durme, J. J., Smits, G., Bonomi, M., Rodien, P., Devor, E. J., Moffat-Wilson, K., Pardo, L., Vassart, G., and Costagliola, S. (2004) *Mol. Endocrinol.* **18**, 2061–2073
39. Shinozaki, H., Fanelli, F., Liu, X., Jaquette, J., Nakamura, K., and Segaloff, D. L. (2001) *Mol. Endocrinol.* **15**, 972–984
40. Corvilain, B., Van Sande, J., Dumont, J. E., and Vassart, G. (2001) *Clin. Endocrinol.* **55**, 143–158
41. Anasti, J. N., Flack, M. R., Froehlich, J., Nelson, L. M., and Nisula, B. C. (1995) *J. Clin. Endocrinol. Metab.* **80**, 276–279
42. Fanelli, F., Themmen, A. P., and Puett, D. (2001) *IUBMB Life* **51**, 149–155
43. Farrens, D. L., Altenbach, C., Yang, K., Hubbell, W. L., and Khorana, H. G. (1996) *Science* **274**, 768–770
44. Salom, D., Lodowski, D. T., Stenkamp, R. E., Le Trong, I., Golczak, M., Jastrzebska, B., Harris, T., Ballesteros, J. A., and Palczewski, K. (2006) *Proc. Natl. Acad. Sci. U. S. A.* **103**, 16123–16128